Crystallization Behavior of Copper Smelter Slag During Molten Oxidation

YONG FAN, ETSURO SHIBATA, ATSUSHI IIZUKA, and TAKASHI NAKAMURA

Copper slag is composed of iron silicate obtained by smelting copper concentrate and silica flux. One of the most important criteria for the utilization of this secondary resource is the recovery of iron from the slag matrix to decrease the volume of dumped slag. The molten oxidation process with crushing magnetic separation appears to be a more sustainable approach and is based on directly blowing oxidizing gas onto molten slag after the copper smelting process. In the current study, using an infrared furnace, the crystallization behavior of the slag during molten oxidation was studied to better understand the trade-off between magnetite and hematite precipitations, as assessed by X-ray diffraction (using an internal standard). Furthermore, the crystal morphology was examined using a laser microscope and Raman imaging system to understand the iron oxide transformation, and the distribution of impurities such as Cu, Zn, As, Cr, and Pb were complemented with scanning electron microscopy and energy dispersive spectroscopy. In addition, the reaction mechanism was investigated with a focus on the oxidation processes.

DOI: 10.1007/s11663-015-0365-3

I. INTRODUCTION

In the copper smelting industry, nearly 30 million tons of smelter slag is estimated to be produced every year in the world.[10] The recent overcapacity of the cement industry in the developed markets has been causing increasingly serious concern, thereby necessitating the urgent utilization of slag. Most of the slag in developing countries is dumped without being fully recycled, which causes serious environmental pollution and is a huge waste of resources.

Copper slag is composed mainly of iron silicates [(Fe, Al, Ca, Mg,)$_x$ SiO$_y$] obtained by smelting copper concentrate and silica flux. One of the most important criteria for the utilization of this secondary resource is the recovery of iron from the slag matrix, which has a concentration of nearly 40 mass pct that could effectively decrease the volume of the dumped slag.

Several lab-scale studies have been performed for recycling iron from copper slag, such as the multistage grinding-mineral process, smelting reduction, sulfation method, and many hydrometallurgical methods.[2]

In the current study, the molten oxidation process followed by crushing and magnetic separation is shown to be a more sustainable approach that is based on directly blowing oxidizing gas onto the molten slag after copper smelting. During this process, most of the nonmagnetic iron components were designed to be transformed into magnetite, which allows selective recovery of iron-bearing and non-iron-bearing slag constituents for specific purposes.

In a previous study,[3] the time–temperature–transformation diagram of copper slag was obtained for the isothermal transformation into magnetite precipitates between 993 K and 1493 K (720 °C and 1220 °C) under the atmosphere of air. Further, it was observed that, under isothermal procedures, high temperature was an effective factor for magnetite incubation or nucleation. Therefore, in the current study, the crystallization behavior during the molten oxidation process was studied to better understand the relationship between magnetite and hematite precipitations. Furthermore, the crystal morphology was examined using a laser microscope and Raman imaging system to understand the iron oxide transformation, and the distribution of impurities such as Cu, Zn, As, Cr, and Pb were complemented with scanning electron microscopy and energy dispersive spectroscopy. In addition, the reaction mechanism was investigated with a focus on the oxidation processes.

II. EXPERIMENTAL

The chemical composition of copper slag from a smelting furnace used in the current study was as follows: T.Fe = 37.9 mass pct, SiO_2 = 35.0 mass pct, Al_2O_3 = 4.6 mass pct, CaO = 2.0 mass pct, MgO = 1.5 mass pct, Zn = 0.96 mass pct, Cu = 0.83 mass pct, S = 0.59 mass pct, Pb = 0.15 mass pct, As = 0.14 mass pct, and Cr = 0.05 mass pct.

YONG FAN, Doctoral Student 3rd Year, is with the Graduate School of Environmental Studies, Tohoku University, 6-6-20 Aramaki-Aza-Aoba, Aoba-Ku, Sendai, 980-8579, Japan. ETSURO SHIBATA and TAKASHI NAKAMURA, Professors, ATSUSHI IIZUKA, Assistant Professor, Institute of Multidisciplinary Research for Advanced Materials (IMRAM), Tohoku University, 2-1-1 Katahira, Aobaku, Sendai, 980-8577, Japan. Contact e-mail: etsuro@tagen.tohoku.ac.jp

Manuscript submitted March 3, 2015.
Article published online May 19, 2015.

Glassy iron silicate was the main component of the water-granulated copper slag studied previously,[3] which was the base and background of slag matrix. There were relevant amounts of matte suspension, and the precipitation of fayalite and magnetite may have resulted from the matte smelting process or water cooling. The magnetite content was 7.5 mass pct in the original water-granulated slag, when analyzed using the chemical titration method.

The simulation of our proposal, which involves directly blowing oxidizing gas onto molten slag for magnetite precipitation, was implemented using the apparatus, as already described in a previous paper.[3] The apparatus consists of an infrared furnace (RHLP410 C, ULVAC-RIKO Inc., Yokohama, Japan), vacuum pump, heating control system, and gas system to accurately simulate the condition of our proposal for the study of crystallization behaviors.

The molten oxidation precipitations were obtained using the following procedures. First, the copper slag sample (300 mg of original copper slag in an alumina boat) was melted rapidly at 1573 K (1300 °C) under vacuum at approximately 60 K/s. Then, the temperature of the melted sample was stabilized at the melting temperature to ensure uniform melting. Subsequently, the gas flow (pure oxygen, air, 1 vol pct of oxygen + nitrogen) was initiated into the tube at 0.5, 1, and 2 L/minutes to initiate the crystallization. After certain duration of heat treatment, the infrared furnace was shut down, and the sample was cooled under vacuum to the room temperature. The vacuum cooling rate can be as rapid as approximately 100 K/s from 1573 K to 1473 K (1300 °C and 1200 °C) to maintain the original state of the copper slag.

The magnetite and hematite contents were measured by X-ray diffraction (XRD; D2 PHASER, 30 kV, 10 mA, Cu-Kα, Bruker, Germany) using the internal standard method proposed by Alexander *et al.*[1] for semi-quantitative analysis. For this analysis, 10.0 mass pct of KCl (99.9 pct, Wako Pure Chemical Industries Ltd., Osaka, Japan) was selected as the internal standard as it produces reasonably simple diffraction patterns and well-defined peaks that do not overlap those in the phase of interest. Standard samples were spiked with different additional magnetite (10 μm, 99.9 pct, Kojundo Chemical Laboratory Ltd., Saitama, Japan) or hematite (3 μm, 99.9 pct, Wako) by weight, and were then homogeneously mixed. The samples were then analyzed by XRD between 20 deg and 80 deg 2θ (Cu). The peaks at 30.1 deg (220) for magnetite; 24.2 deg (012) and 33.3 deg (104) for hematite; and 28.5 deg (200) for KCl were used to establish the calibration line. The concentration of the experimental samples was then calculated by reading the corresponding value from the calibration line.

The size distributions of the powder samples were measured using a laser-scattering particle size measurement apparatus (MT3300II, Microtrac, Japan) valued by "D_{50}," the median, which is defined as the diameter below which half of the population lies.

Typical samples obtained by the different treatment conditions were characterized using a laser microscope (OLS4100, Olympus, Japan), high-speed Raman imaging system (In *Via* Reflex/Stream Line, Renshaw, UK), and scanning electron microscope (SEM; SU-6600, HITACHI, Japan) coupled with an energy-dispersive X-ray spectrometer (EDS; Inca Energy, Oxford, UK).

III. RESULTS AND DISCUSSION

In the copper slag, Fe, Si, and O were the main elements, and represented more than 90 mass pct. Therefore, it is necessary to study the thermodynamic properties based on the phase diagram of Fe-Si-O system as in the framework of our proposal.

Figure 1 shows the phase diagram of the SiO_2-FeO-Fe_2O_3 system. Fayalite is the main component of copper slag, which has a melting temperature of approximately 1478 K (1205 °C). During molten oxidation, the amount of SiO_2 remains constant in the system; therefore, the phase transformation route should be parallel to the FeO-Fe_2O_3 line starting from liquid fayalite slag (Figure 1, A region). As the oxidation continues, the magnetite (Figure 1, B region) and silica (Figure 1, C region) would be precipitated. Moreover, if there was a strong "driving force," the liquid phase would disappear (Figure 1, D region) and hematite would appear (Figure 1, E region). Magnetite, hematite, and silica had higher melting temperatures and would be present as solids at 1573 K (1300 °C). In the current study, the reaction equilibrium states A, B, C, D, and E regions closely corresponded to the "driving force," which was mainly affected by the oxygen partial pressure.

However, the thermodynamic analysis could only clarify a simulation of the reaction equilibrium state. During the oxidation reaction, both magnetite and hematite could be present, and their relationship is still unknown because of the complexity of the reaction mechanism.

A. *Trade-Off Relationship between Magnetite and Hematite*

In the current study, the molten oxidation of fayalite slag into magnetite and hematite in three different gas atmospheres was considered to study their relationship.

Figure 2 presents some typical XRD patterns of copper slag after thermal treatments at different oxygen partial pressures and heat-treatment durations.

The original copper slag (Figure 2, copper slag) contains fayalite and magnetite due to the matte smelting process or water cooling.

The oxygen atmosphere provided a strong oxidation to slag in a short time to produce obvious magnetite, and less intensive hematite peaks were observed. In addition, the fayalite peaks were reduced to become smaller (Figure 2, O_2 1 minute). Together with the increasing heat-treatment duration, the content of hematite was enhanced, whereas that of magnetite was decreased, and the fayalite peaks almost disappeared (Figure 2, O_2 20 minutes).

The samples treated in the air atmosphere were also crystallized to magnetite and hematite. A short-duration

oxidation led to intensive magnetite peaks and weakened fayalite peaks. In addition, small hematite peaks emerged, revealing that the air atmosphere was still highly oxidizing (Figure 2, air 2 minutes). With the increasing duration of oxidation, hematite became the dominant crystal, and magnetite was degraded similar to that for the oxygen atmosphere (Figure 2, air 60 minutes).

The use of 1 vol pct of oxygen with the remainder being nitrogen resulted in selective oxidation ability. Even long-duration heating did not result in the appearance of hematite, and the magnetite was uniquely stable, which indicated that the iron in the slag was selectively oxidized to magnetite (Figure 2, 1 vol pctO_2 + N_2 20 minutes).

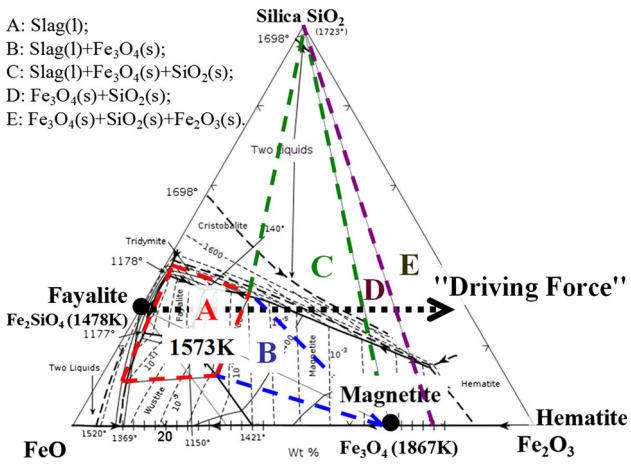

Fig. 1—Phase diagram of SiO_2-FeO-Fe_2O_3 system.[4]

A series of experiments were implemented to semi-quantitatively measure the individual crystal contents using the XRD internal standard method, and the results obtained from different gas atmospheres of molten oxidation are presented in Figures 3, 4, and 5. These results indicate that the mass content variations during the thermal treatment provide evidence of the trade-off relationship between magnetite and hematite.

The pure oxygen atmosphere (Figure 3) led to a rapid increase in the magnetite content in the first minute, which resulted in a magnetite content of nearly 30 mass pct. Then, the magnetite content began to decrease at a diminishing rate to 10 mass pct after a longer duration of oxidation of 40 minutes, whereas the hematite content exhibited the reverse behavior and finally stabilized to approximately 30 mass pct. The gas flow rate contributed to the difference in the transition rate when it surpassed the magnetite content peak.

When the oxygen partial pressure was reduced to the level of air (Figure 4), approximately 6 minutes were required for magnetite precipitation to generate a 40 mass pct peak, while the hematite was growing at a relatively slower rate. After treatment for 60-minute duration, the hematite became the main component of the slag and was stable at approximately 25 mass pct, whereas the magnetite content decreased to less than 20 mass pct. The gas flow rate also affected the transition rate beyond the magnetite content peak.

The use of 1 vol pct of oxygen with the remainder being nitrogen resulted in selective oxidation ability. It was observed that the existing iron oxide was only magnetite, which required approximately 10 minutes to become stable at approximately 50 mass pct. For heat-treatment duration of 1 hour, hematite peaks might have appeared, but their intensity values still remained very low; they were less than the amounts quantified

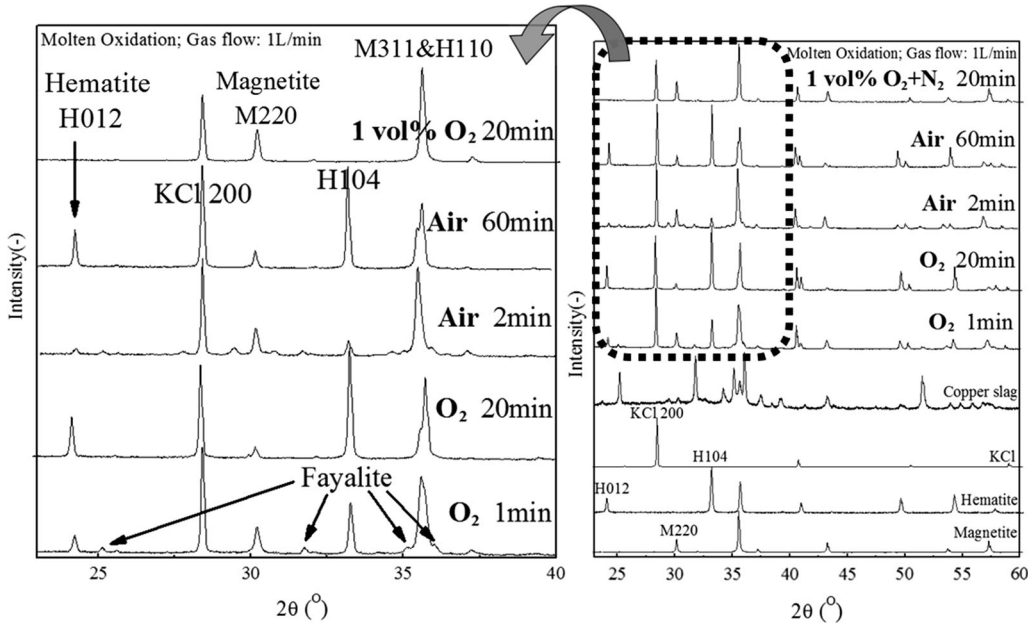

Fig. 2—Typical examples of XRD patterns of copper slag after thermal treatments at different oxygen partial pressures and heat-treatment durations.

using the XRD method. Moreover, the gas flow rate did not show any clear evidence of change in the magnetite formation rate.

Combining these three figures, it can be observed that the oxygen contributed to a rapid increase of magnetite content. When the oxygen partial pressure was decreased to that of air or to 1 vol pct of oxygen, the time taken for the magnetite content to peak increased along with that taken for the maximum content of magnetite to increase, which suggests that lower oxygen partial pressure was beneficial to the precipitation of magnetite. The use of 1 vol pct of oxygen resulted in a selective oxidation tendency, which restrained the growth of hematite. For hematite, a high oxygen partial pressure contributed to more effective hematite production.

B. *Crystal Morphology and Impurity Distribution*

Figures 3, 4, and 5 show the mass content variations of magnetite and hematite during molten oxidation, which reveals the average integral change with time. The study of the crystal morphology, a microscopic level phenomenon, was undertaken to better understand the mechanism of molten oxidation by which the nucleation, growth, and transformation of the crystal phase occurred. Based on many testing results from SEM–EDS, laser microscopy, and Raman spectroscopy, the crystal morphology is illustrated with typical examples.

The laser microscopy images of the copper slag after molten oxidation in a pure oxygen atmosphere for 5 minutes are presented in Figure 6.

This typical cross section of a slag sample subjected to molten oxidation produced four characteristic crystal structures compared with the original copper slag. One structure is a square-like crystal (Figure 6, A); usually, approximately 10 μm occupied the majority of the sample. Another structure is a tower-like crystal (Figure 6, B), which usually clusters together and has a clear square boundary. The third structure is a spindle-like crystal (Figure 6, C), which has thin and long branches extending around it. The final structure is a round crystal (Figure 6, D) usually less than 5 μm; a long oxidation duration was observed to be advantageous for its appearance.

To qualitatively distinguish between the different crystal phases of the iron oxides, micro-area detection was used *via* Raman spectroscopy, which could focus on a small inter space of less than 1 μm, and Raman scattering could distinguish between magnetite and hematite by shift peaks of the wavelength.

Figure 7 shows a typical example. Crystal structures A and B are observed to be magnetite, whereas crystal structures C and D exhibit obvious hematite peaks.

Combined with many other testing results, it was supposed that the square-like crystal is magnetite, and the round crystal is hematite. There was a possible existence of a transition structure from magnetite to hematite; in the current study, the tower- and spindle-like crystals were considered to be these transition structures based on current knowledge.

EDS line scans were obtained to study the changes in the relative amounts of impurities such as Cu, Zn, As, Cr, and Pb in the iron oxides. Combining the results obtained from line scans of many samples, a selective distribution tendency of the impurities was observed.

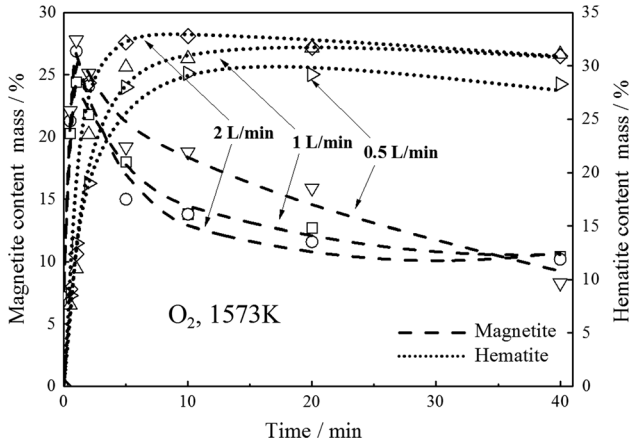

Fig. 3—Variations of the magnetite and hematite contents in copper slag during molten oxidation in pure oxygen atmosphere.

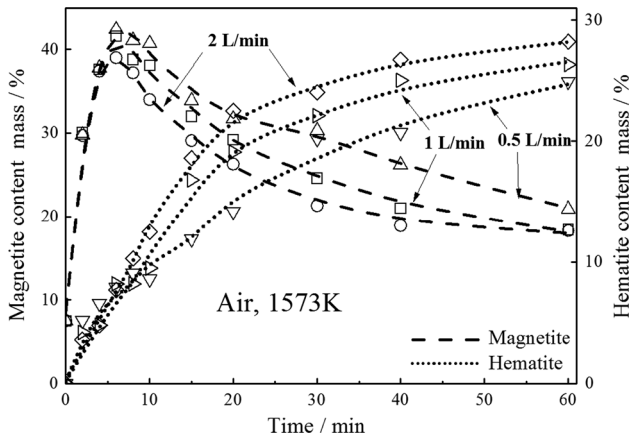

Fig. 4—Variations of the magnetite and hematite contents in copper slag during molten oxidation in air atmosphere.

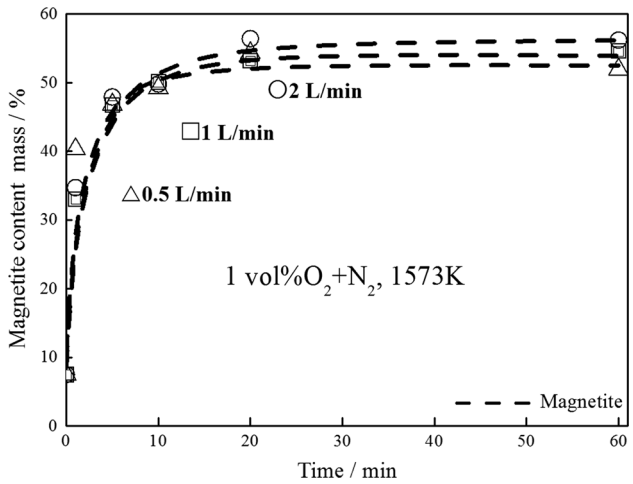

Fig. 5—Variations of the magnetite contents in copper slag during molten oxidation in 1 vol pct O_2 atmosphere.

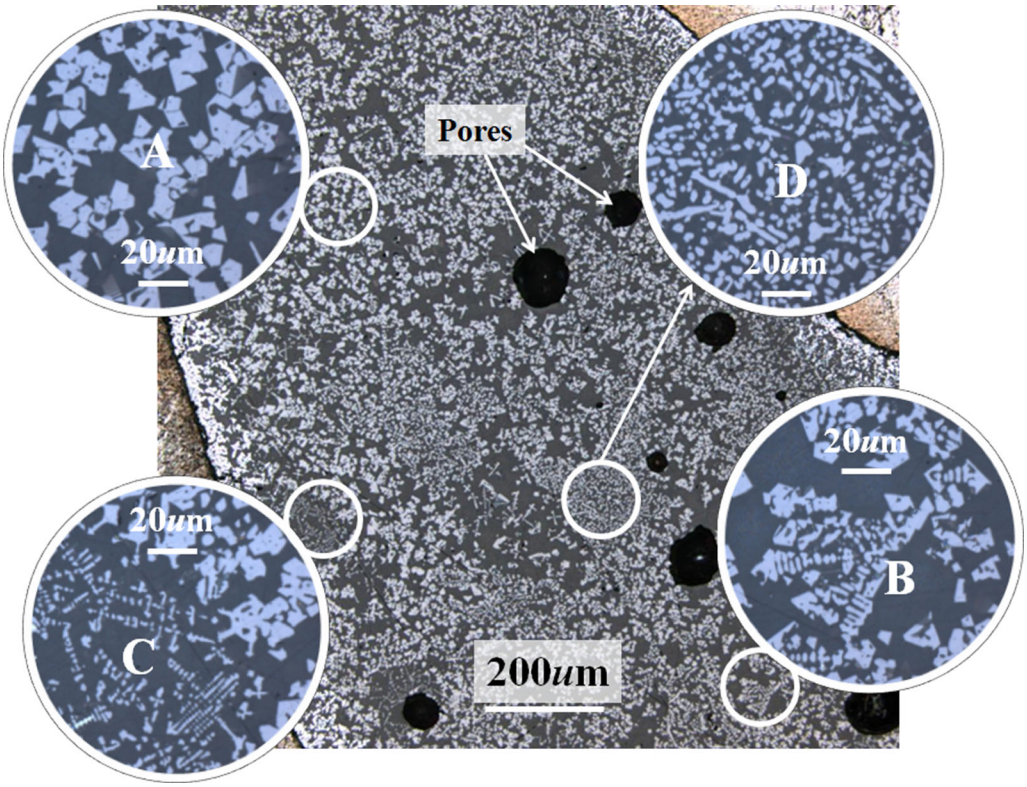

Fig. 6—Typical laser microscopy images of copper slag after molten oxidation in pure oxygen atmosphere for 5 min.

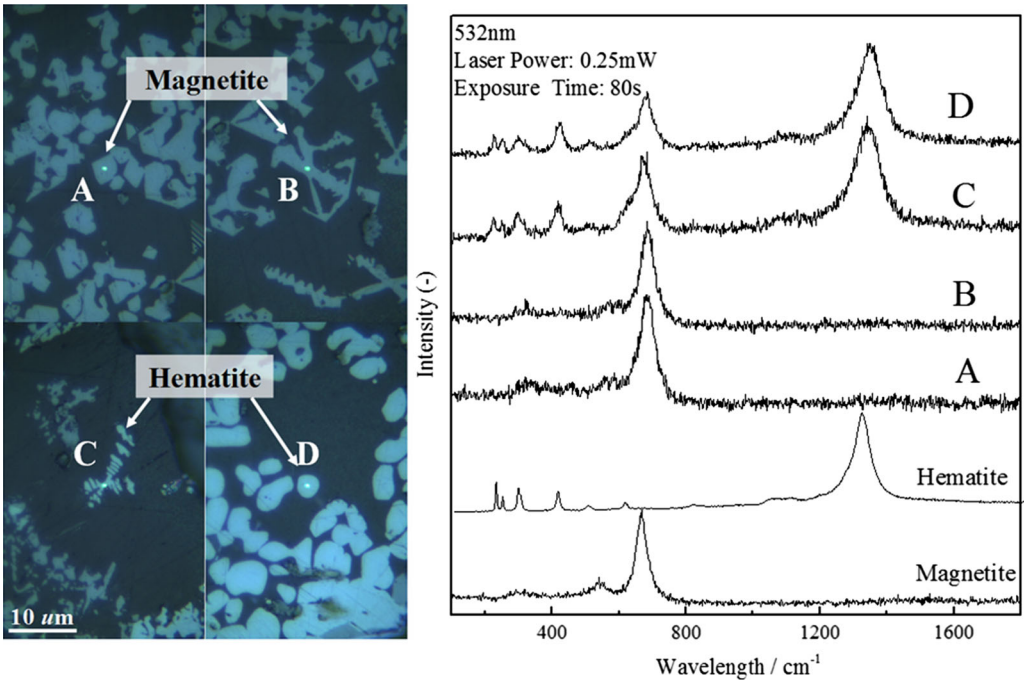

Fig. 7—Typical Raman patterns obtained from micro-area detection of copper slag after molten oxidation in pure oxygen atmosphere for 5 min.

Figure 8 presents a typical analysis; the presence of Cr and Zn shows likelihood of being tracked with Fe and their existence in iron oxides, whereas Cu exhibits the reverse behavior. A relocation tendency of Cu clearly illustrated the Cu shifting out of the crystals. In addition, there is no clear tendency observed for the Pb and As distributions.

C. *Reaction Mechanism*

The iron content in the slag matrix is important because it determines how efficiently iron transfers from the molten iron silicate to the precipitated iron oxides during oxidation.

In Figure 9, the iron content was detected and calculated as the average of at least six values determined by EDS point analysis in the slag shown as the background in the SEM image. Each point data in this figure resulted from one SEM microzone of the slag samples.

As the oxidation time increased, the iron content in the slag matrix decreased. During this decrease, it was supposed that iron was emigrating and transforming into precipitated iron oxides, and silica was saturating in the molten slag and was precipitating.

The study of the trade-off relationship between magnetite and hematite, crystal morphology, and iron-transferring behavior indicated that the change of mechanism as the reaction progressed was complex. It would be interesting to understand the mechanism of molten oxidation at the various stages considering the molten slag at different oxygen partial pressures. Combining all the information discussed previously, the reaction mechanism was integrated based on current knowledge.

The molten oxidation process could take place along the following steps:

(1) Oxygen diffusion occurs from the main gas body to the slag surface.

It was assumed that a boundary layer of gas was present on the surface of the slag. The oxygen partial pressure was different in the main gas body and the slag surface. In the current case, the oxygen partial pressure in the main gas body was kept stable, whereas that on the slag surface was changeable because of the oxidizing reaction occurring.

(2) The oxygen would result in a higher content of Fe^{3+} on the slag surface. The following reaction occurs:

$$2Fe^{2+} + O_2(g) = 2Fe^{3+} + 2O^{2-} \quad [1]$$

Sasabe *et al.*[6–9] proposed that when slags contain iron oxide, the oxygen chemically dissolves as O^{2-} through the exchange of "positive holes" between Fe^{2+} and Fe^{3+}, which can be expressed as follows:

$$Fe^{2+} + \oplus = Fe^{3+} \quad [2]$$

where $\oplus$ represents a positive hole. The mobility of the O^{2-} was assumed by Sayadyaghoubi to be a "driving force," a built-in electric field, set up by mobile charge carriers for the transportation of ionic species in the melt.

Upon increasing the oxidation duration, the scale of Fe^{3+}/Fe^{2+} in the slag melt increased; as a result, the concentration of "positive holes" increased because of the equilibrium constant of the reaction in Eq. [2], such that the O^{2-} diffusion would increase as the oxidation proceeded.

(3) With the existence of Fe^{3+}, magnetite would be formed by Fe^{3+}, Fe^{2+}, and O^{2-} and be precipitated primarily because of its low solubility and be a solid because of its melting point being higher than 1850 K (1577 °C),[5] which can be expressed as follows:

$$2Fe^{3+} + Fe^{2+} + 4O^{2-} = Fe_3O_4(s) \quad [3]$$

During this step, the magnetite began to nucleate and germinate.

(4) Precipitated magnetite in the slag melt would be transformed into hematite because of the ion exchange with Fe^{3+}. The following reaction would occur:

$$Fe_3O_4(s) + 2Fe^{3+} + 2O^{2-} = 2Fe_2O_3(s) + Fe^{2+} \quad [4]$$

This high-temperature solid–liquid phase reaction can be comprehended by the Fe^{3+} in the slag melt taking the place of Fe^{2+} in the magnetite, which would transform into hematite. In the current study, it was assumed that the square-like magnetite changes to round-shaped hematite through the tower- or spindle-like transition structure, as illustrated in Figure 6.

The isolated Fe^{2+} from magnetite would again participate in the oxidation reaction, Eq. [1].

Moreover, silica would be saturated in the molten slag and be precipitated out of the silicate, as observed in Figure 9.

$$SiO_4^{4-} = SiO_2(s) + 2O^{2-} \quad [5]$$

(5) With the continuation of oxidation, a stagnant layer of hematite would be developed at the slag surface and expanded with the oxidation process progressing to the inner part of the melt body.

From the above discussion, it can be concluded that the entire reaction was affected in a complicated manner by many factors such as gas diffusion, chemical reaction, and ion diffusion. The "controlling step" may consist of one or a combination of these steps and could change as the reaction progressed.

At the early stage of the reaction, the ion diffusion, which is assumed to be the mobility of O^{2-}, was relatively feeble and was assumed to be the "controlling step" because of the low scale of Fe^{3+}/Fe^{2+}, which would be enhanced as the oxidation progressed.

Moreover, it was observed that the gas flow rate contributed to the difference in the magnetite/hematite transition rate when it surpassed the magnetite content peak in Figures 3 and 4. Therefore, the gas diffusion was assumed to dominate the "controlling step" at the later stage of reaction because of the increasing ion diffusion.

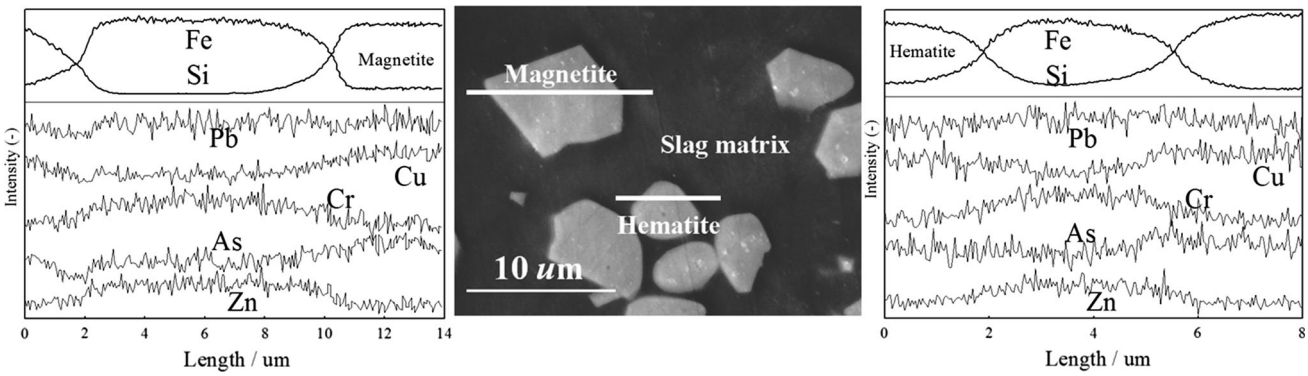

Fig. 8—SEM image and EDS line scan of copper slag after molten oxidation in pure oxygen atmosphere for 1 min.

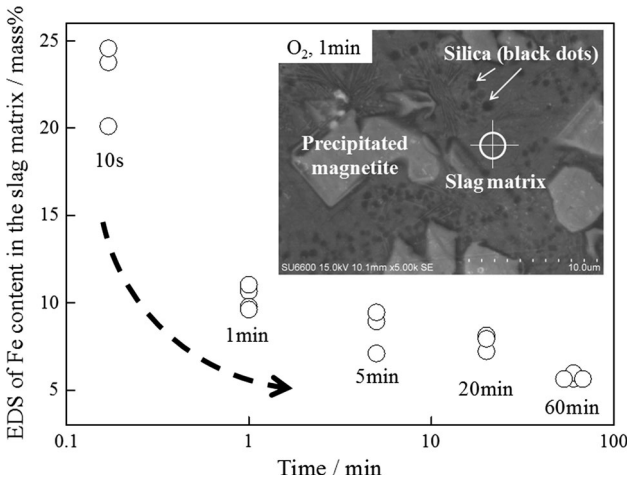

Fig. 9—SEM image and iron content in the slag matrix of samples subjected to molten oxidation in pure oxygen atmosphere.

IV. CONCLUSIONS

In the current study, the simulation of our proposal, which is directly blowing oxidizing gas onto molten slag for magnetite precipitation, was implemented using an infrared furnace. The crystallization behaviors were studied, with the variations of the magnetite and hematite contents during molten oxidation showing a trade-off relationship.

It was concluded that a lower oxygen partial pressure was beneficial to the precipitation of magnetite. In particular, the use of 1 vol pct of oxygen resulted in a selective oxidation tendency for magnetite precipitation.

Moreover, the crystal morphology of the iron oxides and the distribution of impurities were investigated. It was observed that Cr and Zn exhibited likelihood of being tracked with Fe, which emigrated and transformed into precipitated iron oxide during molten oxidation, whereas Cu exhibited the reverse behavior.

In addition, an attempt was made to describe the reaction mechanism considering the molten oxidation processes based on current knowledge. The ion diffusion, which is assumed to be the mobility of O^{2-}, was relatively weak in the early stage and was enhanced as the oxidation progressed. The gas diffusion was assumed to dominate the "controlling step" during the later stage of the reaction.

From the current study, it was found that selective precipitation of magnetite from copper slag could be realized by easily controlling the oxygen partial pressure, which thus sets the foundation for the future studies focusing on highly efficient magnetic separation of iron-bearing and non-iron-bearing slag constituents for specific purposes.

ACKNOWLEDGMENTS

The laser microscope and Raman imaging system used in the current study were provided by the High Efficiency Rare Elements Extraction Technology Area under the Tohoku Innovation Materials Technology Initiatives for Reconstruction from the Ministry of Education, Culture, Sports, Science, and Technology in Japan.

REFERENCES

1. L. Alexander and H.P. Klug: *Anal. Chem.*, 1948, vol. 20, pp. 886–89.
2. Y. Fan, E. Shibata, A. Iizuka, and T. Nakamura: *J. MMIJ*, 2013, vol. 5, pp. 177–84.
3. Y. Fan, E. Shibata, A. Iizuka, and T. Nakamura: *Mater. Trans.*, 2014, vol. 55, pp. 958–963.
4. Phase Equilibria Diagrams Database 31, 2004–2014. The American Ceramic Society and the U.S. Secretary of Commerce.
5. G.V. Samsonov: *The Oxide Handbook*, IFI Plenum, New York, 1982 53.
6. M. Sasabe and Y. Kinoshita: *Iron Steel Inst.*, 1979, vol. 12, pp. 1727–36.
7. M. Sasabe and M. Jibiki: *Iron Steel Inst.*, 1982, vol. 7, pp. 767–73.
8. M. Sasabe and M. Jibiki: *Can. Metall. Q.*, 1983, vol. 22, pp. 29–36.
9. Y. Sayadyaghoubi, S. Sun, and S. Jahanshahi: *Metall. Mater. Trans. B*, 1995, vol. 26B, pp. 795–802.
10. W. Stumm and J.J. Morgan: *World Mineral Production 2007–2011*, Keyworth, Nottingham, 2013.